

Oxidation kinetics of nanocrystalline Al thin films

Jinsong Luo

Key Laboratory of Automobile Materials, Ministry of Education and School of Materials Science and Engineering, Jilin University, Changchun, China; State Key Laboratory of Luminescence and Applications, Changchun Institute of Optics, Fine Mechanics and Physics, Chinese Academy of Sciences, Changchun, China

Ligong Zhang, Haigui Yang and Nan Zhang

State Key Laboratory of Luminescence and Applications, Changchun Institute of Optics, Fine Mechanics and Physics, Chinese Academy of Sciences, Changchun, China

Yongfu Zhu

Key Laboratory of Automobile Materials, Ministry of Education and School of Materials Science and Engineering, Jilin University, Changchun, China

Xingyuan Liu

State Key Laboratory of Luminescence and Applications, Changchun Institute of Optics, Fine Mechanics and Physics, Chinese Academy of Sciences, Changchun, China, and

Qing Jiang

Key Laboratory of Automobile Materials, Ministry of Education and School of Materials Science and Engineering, Jilin University, Changchun, China

Abstract

Purpose – This paper aims to study the oxidation kinetics of the nanocrystalline Al ultrathin films. The influence of structure and composition evolution during thermal oxidation will be observed. The reason for the change in the oxidation activation energy on increasing the oxidation temperature will be discussed.

Design/methodology/approach – Al thin films are deposited on the silicon wafers as substrates by vacuumed thermal evaporation under the base pressure of 2×10^{-4} Pa, where the substrates are not heated. A crystalline quartz sensor is used to monitor the film thickness. The film thickness varies in the range from 30 to 100 nm. To keep the silicon substrate from oxidation during thermal oxidation of the Al film, a 50-nm gold film was deposited on the back side of silicon substrate. Isothermal oxidation studies of the Al film were carried out in air to assess the oxidation kinetics at 400-600°C.

Findings – The activation energy is positive and low for the low temperature oxidation, but it becomes apparently negative at higher temperatures. The oxide grains are nano-sized, and γ -Al₂O₃ crystals are formed at above 500°C. In light of the model by Davies, the grain boundary diffusion is believed to be the reason for the logarithmic oxidation rate rule. The negative activation energy at higher temperatures is apparent, which comes from the decline of diffusion paths due to the formation of the γ -Al₂O₃ crystals.

Originality/value – It is found that the oxidation kinetics of nanocrystalline Al thin films in air at 400-600°C follows the logarithmic law, and this logarithmic oxidation rate law is related to the grain boundary diffusion. The negative activation energies in the higher temperature range can be attributed to the formation of γ -Al₂O₃ crystal.

Keywords Al, Grain boundary diffusion, Nanocrystalline films, Oxidation kinetics

Paper type Research paper

1. Introduction

In the field of engineering materials, with the exception of gold, no pure metals or alloys are stable in air at room temperature. In usual, metals will be oxidized at low temperatures, where the oxidation rate is extremely high at initial time but it becomes

low when a thin oxide scale is formed on the metal base (Suvaci *et al.*, 2000; Zhu *et al.*, 2004). To understand the oxidation behavior of metals, the mechanism for the isothermal oxidation

The current issue and full text archive of this journal is available on Emerald Insight at: www.emeraldinsight.com/0003-5599.htm



Anti-Corrosion Methods and Materials
66/5 (2019) 638–643
© Emerald Publishing Limited [ISSN 0003-5599]
[DOI 10.1108/ACMM-11-2018-2037]

This work was supported by the Key Scientific and Technological Research and Development Project of Jilin Province (20180201080GX), the National Natural Science Foundation of China (No. 61674069 and No. 51631004), the Project of First-Class Universities and First-Class Disciplines, the Fundamental Research Funds for the Central Universities, the Program for Innovative Research Team (in Science and Technology) in University of Jilin Province and the Program for JLU Science and Technology Innovative Research Team (2017TD-09). This research received no external funding.

Received 28 November 2018

Accepted 22 February 2019

of metals has been well established concerning with the scale growth dominated by the atomic diffusion because of the electrochemical potential gradient (Zhu *et al.*, 2004; Gu *et al.*, 2012). Different oxidation rate rules have been reported (Suvaci *et al.*, 2000; Zhu *et al.*, 2004; Weller *et al.*, 2016; Ebinger and Yates, 1998; Hauffe and Kofstad, 1955; Meijering and Verheijke, 1959; Kofstad, 1988). The first one is the linear oxidation rate rule, where the oxidation rate is irrespective to time. Such a rule is controlled by a surface chemisorption or boundary phase reaction in the gas phase (Weller *et al.*, 2016; Ebinger and Yates, 1998). The second one is the parabolic or cubic rule, for which the oxidation rate has an inverse proportion to the square or cubic root of time. In this rule, the rate-determining process is the atomic diffusion through a growing compact oxide scale (Suvaci *et al.*, 2000; Hauffe and Kofstad, 1955; Meijering and Verheijke, 1959). The third one is the logarithmic oxidation rate rule, which usually occurs in the formation of thin oxide films at low or high temperatures (Zhu *et al.*, 2004; Kofstad, 1988). In this case, the reaction is initially quite rapid and then drops off to low or negligible rates, where the rate-determining rate can be attributed to transport of electrons or ions due to electric fields across the oxide film, chemisorption or cavity formation in the film.

As an engineering material, Al has attracted much attention because of its excellent corrosion resistance due to a thin surface layer of aluminum oxide that forms when the bare metal is exposed to air, which effectively prevents further oxidation in a process termed passivation (Vargel, 2004). To facilitate its application, moreover, much work has been done to investigate the thermal oxidation of single-crystal or polycrystalline Al and its oxidation kinetics at relatively high temperatures above 400°C (Zhang *et al.*, 2015; Cai *et al.*, 2014; Boratto *et al.*, 2014; Boratto and de Andrade Scalvi, 2014). Generally, an ultrathin amorphous oxide layer is formed upon heating with limited thickness less than 4 nm, dependent on the oxygen partial pressure (Cai *et al.*, 2014; Reichel *et al.*, 2006; Flötotto *et al.*, 2014; Cai *et al.*, 2012; Lanthony *et al.*, 2012; Reichel *et al.*, 2008a). The oxidation kinetics can be influenced by the temperature, which follows the parabolic oxidation rate rule at around 400°C, the parabolic law between 450 and 600°C, and the asymptotic law at 600°C (Reichel *et al.*, 2008b; Reichel *et al.*, 2006; Libisch *et al.*, 2012; Gulbransen and Wysong, 1947; Smeltzer, 1956). The change in the oxidation kinetics on increasing the temperature is found originated from growth of crystallization in the amorphous thin films. Upon thermal oxidation, for example, the oxides formed on Al above 500°C consist of a thin outer amorphous Al₂O₃ film and inner γ -Al₂O₃ islands (Dignam *et al.*, 1966; Suvaci *et al.*, 2000). As reported by Suvaci *et al.* (2000), Zhu *et al.* (2004) and Wu *et al.* (1993), moreover, relative to the amorphous Al₂O₃ oxides, the oxidation rate of Al can be slowed down upon formation of γ -Al₂O₃ crystals because they are dense free of defects. Owing to this, attention should be paid to the phase transformation in the oxide layers during the Al oxidation.

On the other hand, if the oxide grains formed on metals are nanoscaled, the grain boundary diffusion should be the rate-determining step (Dignam *et al.*, 1966), which may result in a change in the oxidation kinetics in contrast to the polycrystalline case. In previous papers (Hauffe and Kofstad, 1955; Meijering and Verheijke, 1959), attempts have been carried out to study the oxidation kinetics of Cu₂O in the wide temperature range from

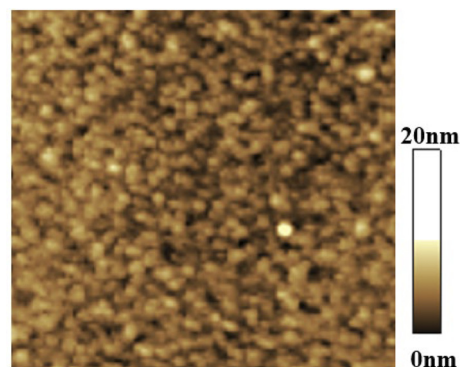
600 to 1050°C, the parabolic or cubic rule was reported for it. More recently, Suvaci *et al.* (2000), Zhu *et al.* (2004) reported that the logarithmic rule was observed for the Cu₂O oxidation, where high activation energy for the Cu₂O oxidation is evaluated at low temperatures, but it becomes low or even negative in the high temperature range. The grain-boundary diffusion is believed responsible for the logarithmic oxidation rule. Relative to the high activation energy at low temperature, the low or negative oxidation activation energies at high temperatures is apparent, which does not mean that the grain boundary diffusion becomes low on increasing the oxidation temperature. Instead, it is essentially attributed to the lateral growth of CuO grains leading to a quick decline of diffusion paths for the transport of reaction species due to the sintering effect. With reference to this, it is necessary to investigate the oxidation kinetics and rules of nanocrystalline Al thin films. However, almost no work has been done to perform it.

In the present paper, an attempt will be made to study the oxidation kinetics of the nanocrystalline Al ultrathin films. The influence of structure and composition evolution during thermal oxidation will be observed. The reason for the change in the oxidation activation energy on increasing the oxidation temperature will be discussed.

2. Materials and methods

Al wires with 99.999 per cent purity as the raw materials are cleaned by alcohol and deionized water, and then they are placed on a tungsten wire. Al thin films are deposited on the silicon wafers as substrates by vacuum thermal evaporation under the base pressure of 2×10^{-4} Pa, where the substrates are not heated. The silicon wafers used in this study are monocrystalline silicon (111), which were purchased from GRINM Semiconductor Materials Co. Ltd. with the specification number of PX-34-0. To achieve a better homogeneity of film, the wafer is kept rotating during the deposition process. The evaporation rate is given at 1 nm per minute controlled by adjusting the current size. A crystalline quartz sensor is used to monitor the film thickness. The film thickness varies in the range from 30 to 100 nm, measured by an Ambios XP-1 surface profile. As shown in Figure 1, the Al thin films are nanocrystalline, composed of nano-sized granules of approximately 10 nm as observed by atomic force microscopy (AFM) (Shimadzu, SPA-9700). To prevent the Al film from being oxidized by the residual water vapor at the starting time during the evaporation process, the baffle is opened after a period of evaporation.

Figure 1 AFM topographical images of as-deposited Al thin films



Note: The scan size is $2 \times 2 \mu\text{m}^2$

To keep the silicon substrate from oxidation during thermal oxidation of the Al film, a 50 nm gold film was deposited on the back side of silicon substrate. Isothermal oxidation studies of the Al film were carried out in air to assess the oxidation kinetics at 400–600°C. A vertical thermo-gravimetric microbalance (HCT-3, China) with an accuracy of 0.1 μg was used to measure the mass gain during oxidation. The oxidation process for Al film was conducted in thermogravimetric analysis (TGA). The samples of Al film, approximately 13 mg, $2 \times 2 \text{ mm}^2$, were placed in a 3-mm diameter and 4-mm deep alumina crucible. They were heated to the oxidation temperature at $10^\circ\text{C}/\text{min}$, and the oxidation is carried out in air for 120 min. The timing of mass gain was started when the furnace reached the oxidation temperature. After oxidation, the specimens were cooled naturally in air. The oxidation kinetics of Al was characterized by the ratio of weight gain to surface area of the Al film.

The surface morphology of the Al films after thermal oxidation at various temperature and duration was observed by AFM. The cross-section morphology was detected by high resolution transmission electron microscope (HRTEM) with an emission voltage of 200 kV (JEOL, JEM-2100F).

3. Results and discussion

3.1 Oxidation kinetics of nanocrystalline Al

In the literatures (Weller *et al.*, 2016; Ebinger and Yates, 1998), Weller *et al.* reported the linear oxidation rate rule for the metal oxidation with:

$$\Delta m = k_0 t + c \quad (1)$$

where Δm is mass gain, t is oxidation time and k_0 and c are constants. To examine if this rule can be met for the oxidation of nanocrystalline Al films, the linear plots of mass gain were plotted for it as shown in Figure 2(a) at 400, 450, 500, 550 and 600°C. However, deviations from the linear rule are observed. In light of this, the oxidation kinetics of nanocrystalline Al does not follow the linear oxidation rate rule. Besides this, the parabolic rule was obtained for the Al oxidation with the bulk size, which is shown as:

$$\Delta m^2 = k_0 t + c \quad (2)$$

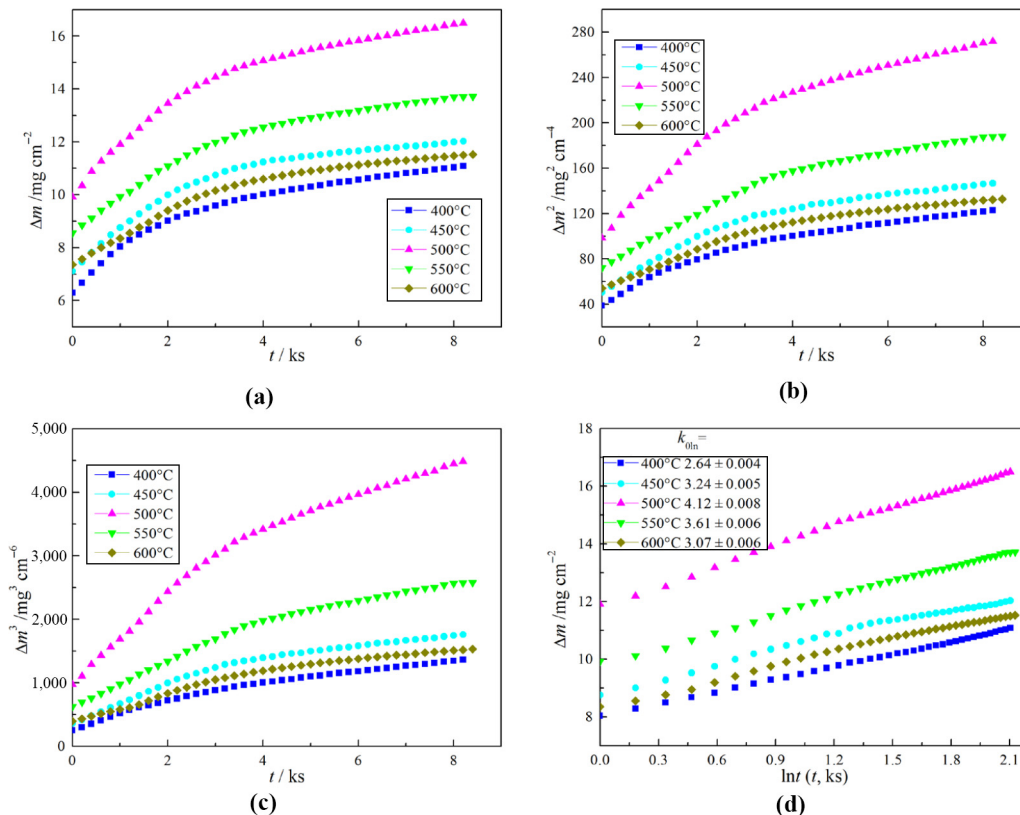
Because of this, the parabolic plots of mass gain for the nanocrystalline Al films were shown in Figure 2(b). However, it deviates from the parabolic rule obviously. Because of this, it shows that the parabolic oxidation rate rule cannot be adopted to elucidate the oxidation kinetics of nanocrystalline Al either.

On the other hand, some researchers (Hauffe and Kofstad, 1955; Meijering and Verheijke, 1959) claimed that the oxidation mass gain of metals obeyed the cubic oxidation rate rule as:

$$\Delta m^3 = k_0 t + c \quad (3)$$

To check it for Al, we here show the mass gain for nanocrystalline Al oxidation with the cubic plots. The typical plots for Al oxidation were shown in Figure 2(c). Deviations from the cubic rule are also observed. This result suggests that, in essence, the cubic oxidation rate rule cannot depict the oxidation kinetics of nanocrystalline Al either.

Figure 2 The mass gain for Al oxidation at 400–600°C plotted with (a) the linear oxidation rule, (b) the parabolic oxidation rule, (c) the cubic oxidation rule and (d) the logarithmic oxidation rule; the constants $k_{0\ln}$ in (d) were obtained from the logarithmic-fitting results of the raw data



Then, the logarithmic function was utilized to fit the mass gain results as:

$$\Delta m = k_{0\ln} \ln(k_{01}t + k_{02}) \quad (4)$$

where $k_{0\ln}$, k_{01} and k_{02} are constants, and k_{01} and k_{02} can be given with the fitting process. Figure 2(d) shows the plots of mass gain data for the Al oxidation from 400 to 600°C as the function of $\ln t$. Interestingly, the mass gain rises linearly as $\ln t$ increases, inferring that the logarithmic rule can be applied to elucidate the oxidation kinetics of nanocrystalline Al. By the fitting method, the logarithmic oxidation rate constants $k_{0\ln}$ are given, which rises from 2.64 to 4.12 $\text{mgcm}^{-2}\text{ks}^{-1}$ at 400–500°C but then decreases to 3.07 $\text{mgcm}^{-2}\text{ks}^{-1}$ at 600°C.

To further understand the oxidation kinetics of nanocrystalline Al films, the Arrhenius plots of the logarithmic oxidation rate constants $k_{0\ln}$ are presented in Figure 3. The slope for the oxidation is positive at 400–500°C, but it becomes negative at

Figure 3 Arrhenius plots of the logarithmic rate constants for Al oxidation at 400–600°C

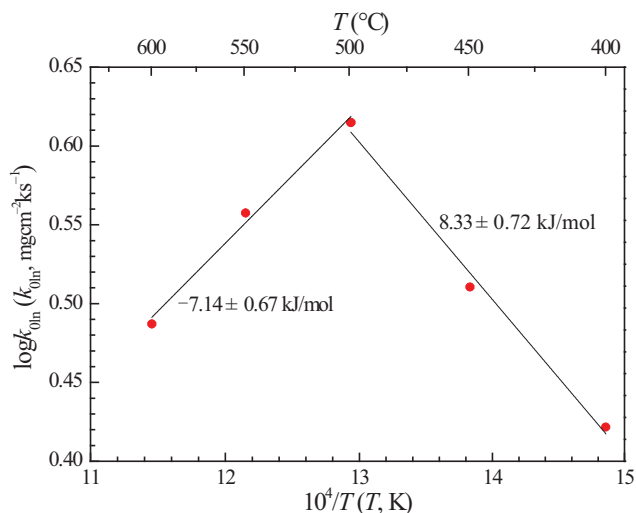
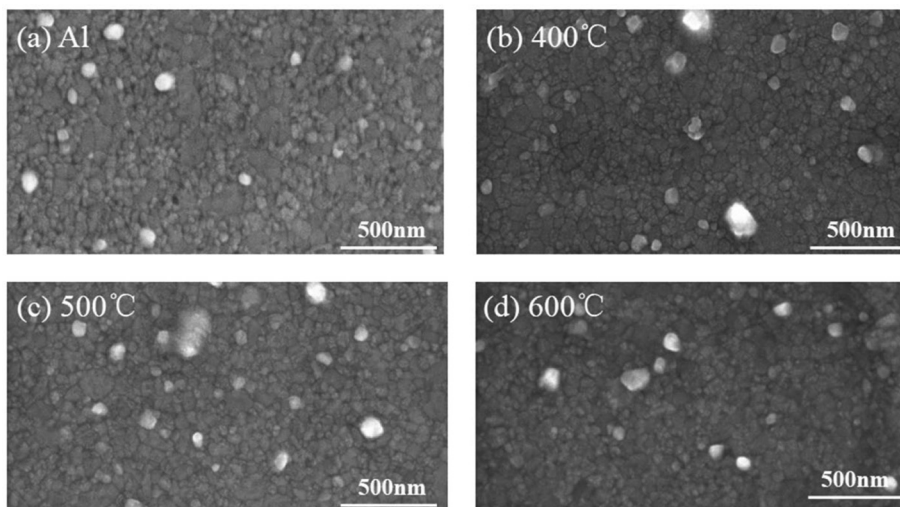


Figure 4 SEM micrographs of Al thin films (a) as-deposited, (b)–(d) thermal oxidation at 400, 500 and 600 °C for 120 min, respectively



500–600°C. In light of the Arrhenius plots, the oxidation activation energy Q_a was assessed and given in Figure 3. Q_a is 8.33 ± 0.718 kJ/mol at 400–500°C, but becomes negative as -7.14 ± 0.67 kJ/mol at 500–600°C. Obviously, the change in Q_a for Al oxidation on increasing the oxidation temperature is consistent with the case of the Cu_2O oxidation investigated by Hauffe and Kofstad (1955), Meijering and Verheijke (1959), Suvaci et al. (2000) and Zhu et al. (2004), although they reported different oxidation rate rules in their works.

Suvaci et al. (2000) reported that, for Al oxidation, the oxidation kinetics obeys the parabolic rate rule, where the grains in Al specimens are large as micrometer in diameter. To investigate the case in this work, the surface morphology of the Al specimens were observed by SEM as shown in Figure 4. Figure 4(a) shows the SEM observation of Al thin film as-deposited with approximately 100 nm thickness. Uniform nanocrystalline films can be observed with spherical particles at several tens of nanometers in size. Figure 4(b)–(d) shows the SEM observation of Al thin films after the thermal oxidation at 400, 500 and 600°C for 120 min. The Al films after oxidation show a similar morphological character in comparison with the as-deposited film, and there seems almost no increase in the grain size on increasing the oxidation temperature.

According to Figure 4, the Al films after oxidation consists of nano-sized grains, much different from the polycrystalline case as reported by Suvaci et al. (2000). It is thus probable that nanocrystalline Al_2O_3 grains should be responsible for the logarithmic rate rule for the oxidation of nanocrystalline Al films, which will be investigated as follows.

3.2 Model for the logarithmic oxidation rate rule

According to the work by Kofstad (1988), the oxidation kinetics of metal at low temperatures could be depicted using the logarithmic rate rule. Davies et al. (1954) proposed that such an oxidation rate rule can be interpreted in a non-uniform process by assuming the progressive blocking of low resistance diffusion paths, such as dislocations or grain boundaries. In this model, it is supposed that the reacting atoms or ions transports mainly along dislocations or grain boundaries, while it can then be blocked or

deactivated when new oxides are formed. The logarithmic oxidation rate rule can then be derived when the neighboring dislocations or grain boundaries paths are blocked by the newly formed fresh oxide because of the compressional stress.

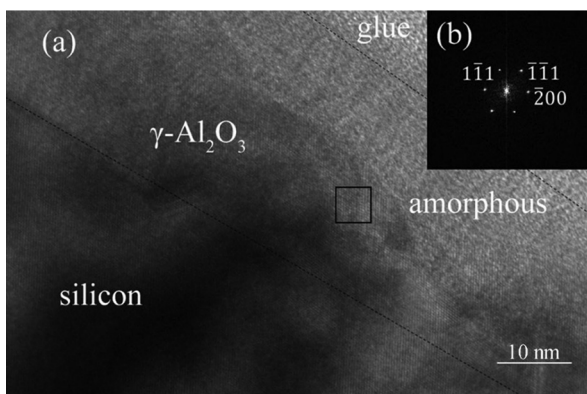
In the present work, the thin Al_2O_3 layer is compact and protective with the pilling-Bedworth ratio of 1.28 (Segawa *et al.*, 2013). Hence, the rate-determining step is believed to be the reaction atoms transport through grain boundaries or defects. Since an increase in volume by nearly 30 per cent occurs for Al transformation to Al_2O_3 , in addition, during the oxidation process, this results in compressive stress in Al_2O_3 film. All these are consistent with the necessary condition of model by Davies *et al.* (1954). Thanks to these, the logarithmic rate rule of Al oxidation can be interpreted by his model.

3.3 Explanation to negative activation energy at higher temperature

In view of the model by Davies *et al.* (1954), the grain boundary or defect diffusion of O atoms and the newly formed Al_2O_3 grains will affect the logarithmic oxidation rate constant. In the present work, considered that the grain boundary diffusion will not be slowed down on increasing the oxidation temperature, the decline of diffusion paths should be responsible for the negative activation energy at 773 - 873 K. As there is almost no increase in the grain size on increasing the oxidation temperature to decrease the diffusion paths as shown in Figure 4, the grain growth should have no contribution to the negative activation energy between 773 and 873 K. Because of this, a decline of diffusion paths for the transport of reaction species due to the appearance of γ crystallite should be considered. Owing to it, we will check the roles played by the phase composition of Al_2O_3 oxides and the grain boundary or defect diffusion on increasing the oxidation temperature.

To observe the existence of γ crystallite, the HRTEM picture of the cross-section of oxide film formed at 500°C for 10 h was given in Figure 5. The Al oxide film involves an outer amorphous layer and an inner crystallite layer. The electron diffraction pattern demonstrated that the crystal particle is a $\gamma\text{-Al}_2\text{O}_3$ crystallite. With the HRTEM technique, in fact, Jeurgens *et al.* (2002) reported that a thick $\gamma\text{-Al}_2\text{O}_3$ was formed at the interface between the initial amorphous oxide film and

Figure 5 (a) HRTEM micrographs of cross-section of an Al film on the silicon substrate heated for 10 h at 500°C; (b) electron diffraction pattern of the $\gamma\text{-Al}_2\text{O}_3$ crystallite located in the black frame of (a), with the direction of the electron beam along $[011]_{\gamma\text{-Al}_2\text{O}_3}$



the silicon substrate for an Al film with 35 nm in thickness on the silicon substrate heated at 500°C for 10 h. This observation confirms that the annealing temperature and time can both play a crucial role in the crystallization process.

Based on the TEM images of the Al films oxidized at different thermal oxidation temperature, the oxidation process should undergo formation of the amorphous layer on the surface and the crystalline under amorphous layer in sequence at above 500°C. In agreement with this, Henry *et al.*, examined the oxidation of clean (111) Al surfaces at 577°C under UHV conditions (Henry *et al.*, 1982). They concluded from the position of the XPS Al(2p) peak that $\gamma\text{-Al}_2\text{O}_3$ was the only oxide present. This result shows that the stoichiometry is 1:1.5 for Al/O, leading to the absence of O defects in the crystalline oxides. As a result, the diffusion of O through the Al_2O_3 oxides will be much slow. The identification of the crystalline nature of the oxide from the position of the XPS Al(2p) peak is, however, ambiguous for the lower temperature oxidation because of the range of peak shifts (Ocal *et al.*, 1985). Such an ambiguity is induced by the deviations in stoichiometry of Al/O, resulting in the presence of Al and O vacancies in the oxides, inducing quick inward diffusion of Al and O atoms in the Al_2O_3 oxides. Owing to these, the formation of $\gamma\text{-Al}_2\text{O}_3$ crystals at high temperatures can slow down the oxidation rate of Al because of its high density free of defects (Suvaci *et al.*, 2000; Zhu *et al.*, 2004), while the diffusion along grain boundaries or defects should be preferential for the low temperature oxidation of the nanocrystalline Al films. As a result, the negative oxidation activation energy at 500-600°C can be interpreted from formation of the $\gamma\text{-Al}_2\text{O}_3$ crystals.

With the molecular-dynamic simulations performed from 27 to 477°C on Al polycrystalline samples, Perron *et al.* (2010) observed that, beyond a first linear regime, the kinetics follows a direct logarithmic law governed by diffusion process and tends to a limiting value corresponding to a thickness of 3 nm. In the present work, the timing of mass gain is started when the furnace reach the oxidation temperature. At this time, more than 3-nm oxide is formed on the surface of Al films. Hence, the linear oxidation rate law was not considered in this work. As for the direct logarithmic law governed by the lattice diffusion process reported by Perron *et al.* (2010), it might be largely relevant to the very thin polycrystalline Al_2O_3 films lower than 3-nm with less grain boundaries, much thinner than the nanocrystalline amorphous films in the present experiment work.

4. Conclusions

The oxidation kinetics of nanocrystalline Al films was investigated at 400-600°C. The oxidation kinetics followed the logarithmic rule, not the linear rule, parabolic rule or the cubic rule. The activation energy for Al oxidation is 8.33 ± 0.718 kJ/mol at 400-500°C, and it becomes -7.14 ± 0.67 kJ/mol at 500-600°C. The oxide grains are nano-sized, and $\gamma\text{-Al}_2\text{O}_3$ crystals are formed at above 500°C. In light of the model by Davies *et al.*, the grain boundary diffusion is believed to be the reason for the logarithmic oxidation rate rule. The negative activation energy at higher temperatures is apparent, which comes from the decline of diffusion paths due to the formation of the $\gamma\text{-Al}_2\text{O}_3$ crystals.

References

- Boratto, M.H. and de Andrade Scalvi, L.V. (2014), "Deposition of Al_2O_3 by resistive evaporation and thermal oxidation of Al to be applied as a transparent FET insulating layer", *Ceramics International*, Vol. 40 No. 2, pp. 3785–3791.
- Boratto, M.H., de Andrade Scalvi, L.V. and de Oliveira Machado, D.H. (2014), " Al_2O_3 obtained through resistive evaporation for use as insulating layer in transparent field effect transistor", *Advanced Materials Research*, Vol. 975, pp. 248–253.
- Cai, J., Li, Y., Wu, J.-m. and Ling, G.-p. (2014), "Preparation of self-healing $\alpha\text{-Al}_2\text{O}_3$ films by low temperature thermal oxidation", *Oxidation of Metals*, Vol. 81 Nos 1/2, pp. 253–265.
- Cai, N., Zhou, G., Müller, K. and Starr, D.E. (2012), "Temperature and pressure dependent mott potentials and their influence on self-limiting oxide film growth", *Applied Physics Letters*, Vol. 101 No. 17, p. 171605.
- Davies, D.E., Evans, U.R. and Agar, J.N. (1954), "The oxidation of iron at 175 to 350° C", *Proceedings of the Royal Society of London Series A*, Vol. 225 No. 1163, pp. 443–462.
- Dignam, M.J., Fawcett, W.R. and Böhni, H. (1966), "The kinetics and mechanism of oxidation of superpurity aluminum in dry oxygen", *Journal of the Electrochemical Society*, Vol. 113 No. 7, pp. 656–662.
- Ebinger, H.D., J.T. and Yates, J. (1998), "Electron-impact-induced oxidation of Al(111) in water vapor: relation to the Cabrera-mott mechanism", *Physical Review B*, Vol. 57 No. 3, pp. 1976–1984.
- Flötotto, D., Wang, Z.M., Jeurgens, L.P.H. and Mittemeijer, E.J. (2014), "Intrinsic stress evolution during amorphous oxide film growth on Al surfaces", *Applied Physics Letters*, Vol. 104 No. 9, p. 91901.
- Gu, L., Zou, B., Fan, X., Zeng, S., Chen, X., Wang, Y. and Cao, X. (2012), "Oxidation behavior of plasma sprayed Al@NiCr with cyclic thermal treatment at different temperatures", *Corrosion Science*, Vol. 55, pp. 164–171.
- Gulbransen, E.A. and Wysong, W.S. (1947), "Thin oxide films on aluminum", *The Journal of Physical and Colloid Chemistry*, Vol. 51 No. 5, pp. 1087–1103.
- Hauffe, K. and Kofstad, P. (1955), "Über den Mechanismus der Oxidation von Cu_2O bei hohen Temperaturen", *Zeitschrift für Elektrochemie*, Vol. 59 No. 5, pp. 399–404.
- Henry, R.M., Walker, B.W. and Stair, P.C. (1982), "A blue colored surface observed during high temperature oxidation of aluminum (111)", *Solid State Communications*, Vol. 42 No. 1, pp. 23–26.
- Jeurgens, L.P.H., Sloof, W.G., Tichelaar, F.D. and Mittemeijer, E.J. (2002), "Structure and morphology of aluminium-oxide films formed by thermal oxidation of aluminium", *Thin Solid Films*, Vol. 418 No. 2, pp. 89–101.
- Kofstad, P. (1988), *High Temperature Corrosion*, Elsevier Science Publishing Co., Inc., New York, NY, p. 148.
- Lanthy, C., Ducere, J.M., Djafari Rouhani, M., Hemeryck, A., Esteve, A. and Rossi, C. (2012), "On the early stage of aluminum oxidation: an extraction mechanism via oxygen cooperation", *The Journal of Chemical Physics*, Vol. 137 No. 9, p. 094707.
- Libisch, F., Huang, C., Liao, P., Pavone, M. and Carter, E.A. (2012), "Origin of the energy barrier to chemical reactions of O_2 on Al(111): evidence for charge transfer, not spin selection", *Phys Rev Lett*, Vol. 109 No. 19, p. 198303.
- Meijering, J. and Verheijke, M. (1959), "Oxidation kinetics in the case of ageing oxide films", *Acta Metallurgica*, Vol. 7 No. 5, pp. 331–338.
- Ocal, C., Basurco, B. and Ferrer, S. (1985), "An ISS-XPS study on the oxidation of Al (111); identification of stoichiometric and reduced oxide surfaces", *Surface Science*, Vol. 157 No. 1, pp. 233–243.
- Perron, A., Garruchet, S., Politano, O., Aral, G. and Vignal, V. (2010), "Oxidation of nanocrystalline aluminum by variable charge molecular dynamics", *Journal of Physics and Chemistry of Solids*, Vol. 71 No. 2, pp. 119–124.
- Reichel, F., Jeurgens, L.P.H. and Mittemeijer, E.J. (2006), "Thermodynamic model of oxide overgrowth on bare metals: relaxation of growth strain by plastic deformation", *Physical Review B*, Vol. 74 No. 14, p. 144103.
- Reichel, F., Jeurgens, L.P.H. and Mittemeijer, E.J. (2008a), "The thermodynamic stability of amorphous oxide overgrowths on metals", *Acta Materialia*, Vol. 56 No. 3, pp. 659–674.
- Reichel, F., Jeurgens, L.P.H., Richter, G. and Mittemeijer, E.J. (2008b), "Amorphous versus crystalline state for ultrathin Al_2O_3 overgrowths on Al substrates", *Journal of Applied Physics*, Vol. 103 No. 9, p. 93515.
- Segawa, H., Okano, H., Wada, K., Inoue, S. and Byun, I. (2013), "Synthesis of laminated alumina films by AC oxidation", *Journal of the Electrochemical Society*, Vol. 160 No. 6, pp. D240–D45.
- Smeltzer, W.W. (1956), "Oxidation of aluminum in the temperature range 400°–600°C", *Journal of the Electrochemical Society*, Vol. 103 No. 4, pp. 209–214.
- Suvaci, E.G. and Simkovich Messing, G.L. (2000), "The reaction-bonded aluminum oxide process: i, the effect of attrition milling on the solid-state oxidation of aluminum powder", *Journal of the American Ceramic Society*, Vol. 83 No. 2, pp. 299–305.
- Vargel, C. (2004), *Corrosion of Aluminium*, Elsevier.
- Weller, K., Wang, Z.M., Jeurgens, L.P.H. and Mittemeijer, E.J. (2016), "Oxidation kinetics of amorphous Al x Zr 1–x alloys", *Acta Materialia*, Vol. 103, pp. 311–321.
- Wu, S., Holz, D. and Claussen, N. (1993), "Mechanisms and kinetics of reaction-bonded aluminum oxide ceramics", *Journal of the American Ceramic Society*, Vol. 76 No. 4, pp. 970–980.
- Zhu, Y., Mimura, K. and Isshiki, M. (2004), "Oxidation mechanism of Cu_2O to CuO at 600–1050°C", *Oxidation of Metals*, Vol. 62 Nos 3/4, pp. 207–221.
- Zhang, M., Xu, B. and Ling, G. (2015), "Preparation and characterization of $\alpha\text{-Al}_2\text{O}_3$ film by low temperature thermal oxidation of Al_8Cr_5 coating", *Applied Surface Science*, Vol. 331, pp. 1–7.

Corresponding author

Yongfu Zhu can be contacted at: yfzhu@jlu.edu.cn

For instructions on how to order reprints of this article, please visit our website:

www.emeraldgroupublishing.com/licensing/reprints.htm

Or contact us for further details: permissions@emeraldinsight.com